Electric field-decoupled electroosmotic pump for microfluidic devices

Shaorong Liu*, Qiaosheng Pu, Joann J. Lu

Department of Chemistry and Biochemistry, Texas Tech University, Lubbock, TX 79409, USA

Abstract

An electric field-free electroosmotic pump has been constructed and its pumping rate has been measured under various experimental conditions. The key component of the pump is an ion-exchange membrane grounding joint that serves two major functions: (i) to maintain fluid continuity between pump channels and microfluidic conduit and (ii) to ground the solution in the microfluidic channel at the joint through an external electrode, and hence to decouple the electric field applied to the pump channels from the rest of the microfluidic system. A theoretical model has been developed to calculate the pumping rates and its validity has been demonstrated.
© 2003 Elsevier B.V. All rights reserved.

Keywords: Microfluidics; Instrumentation; Pumps; Chip technology; Electroosmotic flow

1. Introduction

The use of electric field-decoupled electroosmotic pumps for chemical reaction and separation in capillary systems was reported in the literature in the early 1990s [1,2]. This category of pumps has subsequently been introduced to the practice of flow injection analysis (FIA) and other flow analysis systems [2–5]. Electroosmotic flow (EOF) generated from packed capillaries has also been used to pump fluids in small capillary channels. Pressures in excess of 8000 p.s.i. (1 p.s.i.=6894.76 Pa) have been achieved using silica capillaries packed with micron-size silica beads [6,7]. Such an EOF pump has been applied to a micro-bore HPLC system [7].

Fluid manipulations on microfluidic chips are usually achieved using EOF generated in the fluidic channels [8–11], but none of these attempts has been

fully satisfactory. The main reason is that EOF tends to fluctuate after microfluidic channels are exposed to various chemical solutions. For complex fluidic conduits, Kirkoff's law is usually used to determine the flow directions and distributions at intersections. It is challenging to precisely predict and control the flow when EOF fluctuates.

Low-voltage EOF pumps have been reported using a cascade of shallow (0.1–10 μm) channels [12]. A pressure of 500 mmH$_2$O (<1 p.s.i.; 1 mmH$_2$O= 9.80665 Pa) was obtained at 40 V using a 120-nm-gap single stage pump, and it was confirmed that the pressure increased with cascade stage numbers without accumulating voltage. A short segment of gel was photo-polymerized in the chip channel to serve as an electric contact. The cascade configuration combined a group of shallow channels to a relatively deep channel alternatively to increase the pump pressure under a constant operation voltage.

A multiple open-channel electroosmotic pumping system has recently been reported for microfluidic

*Corresponding author. Fax: +1-806-742-1289.
E-mail address: shaorong.liu@ttu.edu (S. Liu).

sample handling [13,14]. The first version of this pump contained some small parallel channels connected to some large parallel channels [13]. In the second version, a porous glass disk was included in the pumping system [14] which consists of hundreds of parallel microchannels 1–6 μm deep and 4–50 mm long and occupies a few square millimeters of chip space. Pressure up to 80 p.s.i. was generated at a flow rate of 17 nl/min. This pump has been used to deliver peptide samples for electrospray ionization mass spectrometric detection [14]. However, it was observed that the pump currents decreased after the porous glass disk was incorporated because some voltage had dropped across the glass disk [14]. This voltage across the glass disk was automatically applied to the rest of the fluidic system and therefore, the fluidic system was not really electric field-free. Additionally, 10–15 min was required for the pump current to be stabilized [14] and this behavior will limit its applications.

We report here a stand-alone electroosmotic pump whose electric field is completely decoupled from the rest of the fluidic conduit. The key component of this pump is an ion-exchange membrane joint that maintains fluid continuity between pumping channels and microfluidic conduit, and permits grounding of the solution in the microfluidic channel at the joint through an external electrode and, therefore, decouples the pump electric field from the microfluidic conduit. Since the pump is fabricated on a microchip, it is readily integrated with any microchip devices. A theoretical model has been developed to calculate the pumping rates and its validity has been demonstrated under various experimental conditions.

2. Experimental

2.1. Photomask design

Fig. 1 presents the photomask design for this experiment. The photomask is designed in house using AutoCat software and produced by LSI Photomask (Phoenix, AZ, USA). Pump channel groups c, d, e, f, g and h, respectively, have 1, 2, 4, 8, 16 and 32 pump channels, all channels having the same length (75 mm). Groups h, i, b, j and a have the same number (32) of pump channels while their lengths
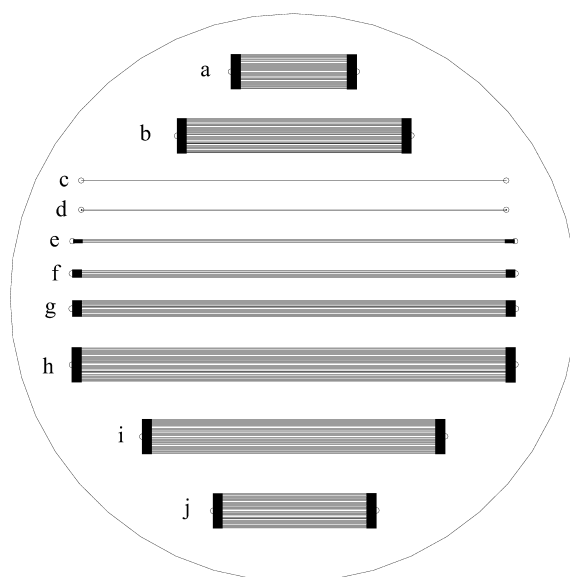

Fig. 1. Photomask design for fabrication of various pump channels. Channel groups c, d, e, f, g and h have 1, 2, 4, 8, 16, and 32 pump channels, respectively. Channels in each group are evenly distributed, but they sometimes look unevenly distributed in this figure due to artifacts when AutoCat files are converted to Microsoft Word documents. Channels in these groups have the same length of 75 mm. Each of the channel groups h, i, b, j and a contains 32 pump channels. Pump channels in these groups have lengths of 75, 50, 37.5, 25 and 18.75 mm, respectively. The ends of the pump channels in each group are combined by a short and fat channel and then connected to the reservoirs. The photomask line-widths of all the pump channels are 100 μm. The center-to-center distance between adjacent channels within a channel group is 200 μm. All pump channels in each group are evenly distributed. The large circle is not part of the photomask lines and is used only to show the size of a 10-cm-diameter wafer.

are 75, 50, 37.5, 25 and 18.75 mm, respectively. For every channel group with more than two pump channels, the ends of the pump channels are combined by a short (1500 μm) and wide (the combined width of all the pump channels and gaps in between the pump channels in the group, as illustrated in Fig. 1) channel that is connected to a reservoir. The photomask line-widths of all the pump channels are 100 μm. The center-to-center distance between adjacent channels within a channel group is 200 μm.

2.2. Microfabrication

The pump channels were microfabricated on 1.1-

mm-thick and 10-cm-diameter borofloat glass wafers (Precision Glass and Optics, Santa Ana, CA, USA) using a fabrication process that has been described previously [15]. Briefly, a borofloat glass wafer was pre-etched in concentrated HF, and then layers of Cr and Au were sputtered on it. The wafer was spin-coated with a thin layer of photoresist (Shipley, Santa Clara, CA, USA) and soft-baked. The photoresist was patterned with UV light through a photomask having the channel patterns as shown in Fig. 1. The photoresist was developed and the exposed Cr/Au was etched off using gold and chromium etchants. The channel pattern was chemically etched into the glass with concentrated hydrofluoric acid. The residual photoresist and Cr/Au were stripped off and access holes were drilled using a diamond drill bit. After a final cleaning in H_2SO_4/H_2O_2, the etched wafer was thermally bonded with a blank wafer. The bonded chip was then diced into pieces containing various numbers of pumping channels as presented in Fig. 1.

2.3. Measurement of the channel dimensions

After grooves were etched on a wafer, their depths and widths were measured on a Tencor α-Step 200 profilometer (KLA-Tencor, San Jose, CA, USA).

The channel width was calculated by averaging the top groove width and the photomask line-width of that groove. The groove depths were taken as the channel depths. All pump channels in the same chip were assumed to have the same depth since the grooves were etched under the same conditions.

2.4. Configuration of electric field-decoupled electroosmotic pumps

Fig. 2a presents the configuration of the pump. Two pipettor tips were cut properly, inserted into the access holes and secured in position using 5-min epoxy glue. A whole pipettor tip was inserted into one of these pipettor tips on the chip to increase its volume and form the high-voltage (HV) electrode reservoir. A polypropylene T-connector was connected to one end of the female part of an HPLC union, and sealed and secured in place with 5-min epoxy glue. Referring to Fig. 2a, a piece of Nafion membrane (DuPont, Wilmington, DE, USA) was tightened to the bottom of the threaded hole of the union with a hollow plastic screw. The hollow space in the screw was used as a ground electrode reservoir. A backpressure capillary (the "pump load") was inserted into another pipettor tip and sealed/secured in position with glue. This pipettor tip was
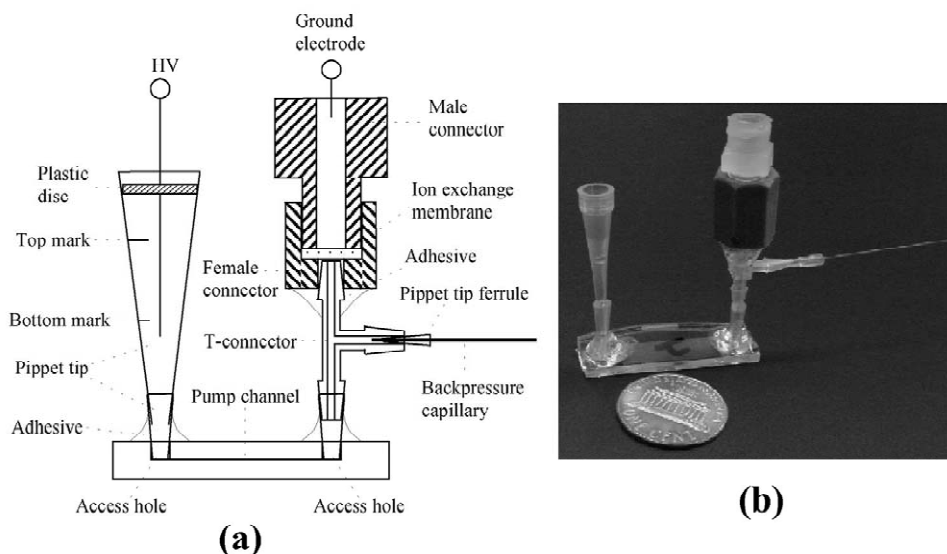

Fig. 2. Assembly of the EOF-based pump. (a) Schematic diagram of the pump configuration and (b) a picture of an assembled pump. The device in the picture contains 32 pump channels and the pump channel length is 18.75 mm.

then inserted into the third end of the T-connector as depicted in Fig. 2a. After buffer solution was filled on both sides of the membrane, the entire assembly was inserted into the other pipettor tip on the chip to form the grounding membrane joint. Fig. 2b presents a picture of the assembled pump. The penny coin in the picture shows the scale of the pump.

2.5. Preparation of pump solutions

Sodium tetraborate solutions were used as pump solutions throughout the experiment. They were prepared by dissolving a proper amount of sodium tetraborate decahydrate powder (Fisher Scientific) in de-ionized water without any pH adjustment. The pH of the solution was measured to be ~9.2. A 2-mM sodium tetraborate solution was used in all experiments except that of Fig. 8.

2.6. Pumping rate measurement

Before each test, the pump solution was filled into all pump channels and reservoirs and a high voltage was applied briefly so that the pump solution came out of the backpressure capillary. The solution on the outlet end of the backpressure capillary was removed and the capillary was inserted into the water in a 1.5-ml-vial through a small hole on the vial cap. The vial, along with the water in it, was weighed before the capillary was inserted. After a proper amount of pump solution was added to (or removed from) the high voltage electrode reservoir until the solution level reached the top mark on the reservoir, the platinum electrode was put into the pump solution. A high voltage was applied between the HV and ground electrode reservoirs until the solution level in the HV electrode reservoir approximately reached the bottom mark on the reservoir. The vial, along with the solution in it, was weighed again. The weight difference was then converted to volume, assuming that 1 mg of the pump solution equals 1-μl volume. The pumping rate was calculated by dividing the converted solution volume by the time for which the high voltage was applied.

2.7. Pump current measurement

A 1-kΩ resistor was inserted (serially) into the circuit directly before the ground electrode when a high voltage was applied to the pump channel(s). During the pump operation, the voltage across the resistor was monitored and recorded, and then converted to the pump current (1 V on the resistor equals 1-mA pump current).

3. Theoretical consideration of EOF pumping

The linear velocity (v_{eo}) of EOF in a narrow channel is generally expressed [16] by:

$$v_{eo} = \frac{\varepsilon \zeta V}{4 \pi \eta L'} \tag{1}$$

where ε is the dielectric constant of the buffer solution, ζ the zeta potential, V the voltage applied across the channel, η the viscosity constant of the pump solution, and L' the length of the pump channel.

Since plug flows are observed in microfabricated channels, the EOF flow rate (Q_{eo}) of a group of parallel channels can be expressed by:

$$Q_{eo} = \frac{n \varepsilon \zeta V w d'}{4 \pi \eta L'} \tag{2}$$

where n is the number of the parallel channels, and w and d', respectively, the width and depth of the microfabricated channel.

Referring to Fig. 2, as a backpressure capillary is connected to the pump channels, the EOF generated from the pump channels will drive the solution in the capillary forward and an internal pressure (Δp) at the junction will be created. Based on the Hagen-Poiseuille equation [17], the flow rate in the capillary (Q_c) is described as:

$$Q_c = \frac{-\pi(\Delta p)d^4}{128 \eta L} \tag{3}$$

where d and L are, respectively, the diameter and length of the backpressure capillary. The negative sign means the flow direction is always from higher to lower pressure.

This internal pressure also makes the solution in the microfabricated channels flow backwards. Because the width of the pump channel is much greater than its depth, flow in such a channel can be treated

as flow in two parallel planes. The total backward flow rate (Q_b) of n parallel pump channels can be described [18] as:

$$Q_b = n \int_0^{\frac{d'}{2}} 2wudx = \frac{-nw(\Delta p)d'^3}{12\eta L'} \tag{4}$$

Combination of Eqs. 3 and 4 gives,

$$Q_c = \frac{3\pi L' d^4 Q_b}{32nLwd'^3} \tag{5}$$

Because both Q_c and Q_b originate from Q_{eo}, and based on the incompressibility continuity hypothesis of liquid fluids,

$$Q_{eo} = Q_c + Q_b \tag{6}$$

Combination of Eqs. 2, 5 and 6 gives,

$$Q_c = \frac{3n\varepsilon\zeta Vwd'd^4}{4\eta(3\pi L'd^4 + 32nLwd'^3)} \tag{7}$$

4. Results and discussion

The channels that combined the pump channels and connected them to reservoirs were made short and wide to reduce their flow resistances and the voltages dropped across them. These channels contributed to less than 0.5% of the total flow and electric resistance and, therefore they were neglected in the theoretic model development and the following discussion. A 1 kΩ resistor was used to facilitate the pump current measurement. The voltage drop across this resistor was less than 1 V and so this voltage was also neglected in the following discussion.

In the flow-rate measurement, the liquid level in the HV electrode reservoir varies slightly with time. This change causes some hydrostatic pressure across the pump channels. To test whether this hydrostatic pressure (<7 mmH$_2$O) affects the flow rate, the HV electrode reservoir was replaced with a 10-mm-diameter reservoir. The liquid level in this reservoir remained virtually the same after several microliters of pump solution was pumped out. No distinguishable flow-rate difference was observed before or after the HV electrode reservoir was changed.
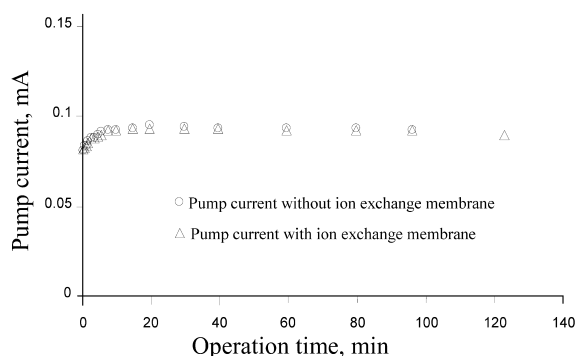

Fig. 3. Pump current as a function of operation time. The pump device used in this experiment contains 32 pump channels. Each pump channel has a length of 75 mm, a width of 127 μm, and a depth of 15.5 μm. The pump solution is a 2-m*M* sodium tetraborate solution. No backpressure capillary is attached to the pump. A voltage of 5 kV is applied across the pump channels. The operation time is the duration when the voltage is applied.

The stability of the electric current through pump channels is often considered a reflection of the stability of the pumping rate. Fig. 3 presents the pump currents as a function of operation time. Due to Joule heating, the pump current increased from 82 to 90 μA within the first 3–4 min. Afterwards, the pump current became very stable and the standard deviation of the current fluctuation was less than ±1%. Once the Joule heating and heat dissipation of the chip reached an equilibrium, the current jumped to the stable current promptly when the pump was briefly stopped and then restarted. If the pump was stopped for longer than 1 min, the 3–4-min warming up time was necessary to regain the stable current.

Fig. 3 also presents a comparison of the pump current with (the data points represented by the triangle symbols) and without (the data points represented by the circle symbols) the ion-exchange membrane. These two current–time curves are virtually the same. These results indicate that little voltage is dropped across the ion-exchange membrane and that the electric field applied to the pump channels is really decoupled from the rest of the system.

The data points in Fig. 4 indicate the measured pumping rate, Q_c, at different backpressure-capillary length, L. The solid line is obtained using a least-square regression (Minsq Software, MicroMath, Salt Lake City, UT, USA) with the following equation:
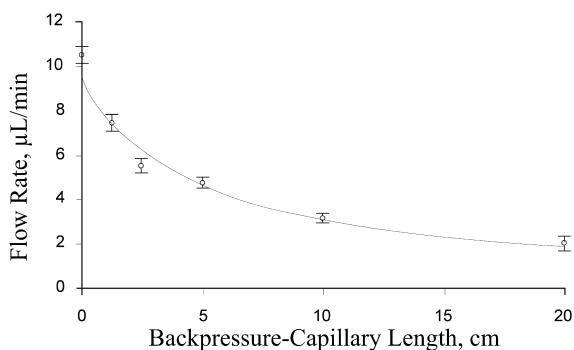
Fig. 4. Effect of backpressure-capillary length on pumping rate. The same pump device used in Fig. 3 is utilized and backpressure capillaries of various lengths are attached to this device for this experiment. All other conditions are the same as those described in Fig. 3. The circular symbols represent the pumping rates measured at various lengths of backpressure capillary. The solid line represents the calculated pumping rate based on Eq. (7).

$$Q_c = \frac{a}{L + b} \tag{8}$$

With the dimensions used in the axes of Fig. 4, the simulation gives: $a = 46.462$, $b = 4.953$, and a correlation coefficient of $r^2 = 0.9961$.

Comparing Eq. (7) with Eq. (8), we have:

$$a = \frac{3\varepsilon\zeta Vd^4}{128\eta d'^2} \tag{9}$$

and

$$b = \frac{3\pi L'd^4}{32nwd'^3} \tag{10}$$

In this experiment, $L' = 7.5$ cm, $d = 75$ μm, $n = 32$, and $w = 127$ μm. Using Eq. (10) and the value of b obtained from the simulation, d' is calculated to be 15 μm. The pump channel (groove) depth measured before the wafers were bonded is 15.5 μm, which indicates a good agreement between the theoretical model and the experimental data.

Meanwhile, the combined constant, $\varepsilon\zeta/\eta$, is calculated to be 0.41 mm^2 V^{-1} s^{-1}, based on Eq. (9), the experimental parameters and the values of d' and a obtained from the simulation. Generally speaking, measuring the exact zeta potential, ζ, is extremely challenging. The method described here provides an alternative way to obtain the zeta potential.

Once the combined constant is obtained, the pumping rates under various experimental conditions can be conveniently calculated using Eq. (7) and compared with the experimentally measured data to further examine the validity of this model. Figs. 5, 6 and 7 present the pumping rates as a function of the voltage applied across the pump channels, the length of the pump channel, and the number of pump channel, respectively. In Fig. 6, the same field strength, more precisely a constant current, was maintained when the channel lengths were varied. The data points in each figure represent the measured pumping rates and the solid line represents the calculated number based on Eq. (7). The measured flow rated matched the theoretically predicted number very well.

Many other factors, such as pH, ionic concentration, temperature, viscosity, dielectric constant and impurities of the pump solution, can also change the pumping rate through affecting the EOF. Fig. 8 demonstrates the effect of the sodium tetraborate concentration on EOF. Because zeta potential usually decreases with the salt concentrations in the solution, the EOF decreased with sodium tetraborate concentration in Fig. 8. The EOF of water was the lowest because water has a low pH (pH 7) compared
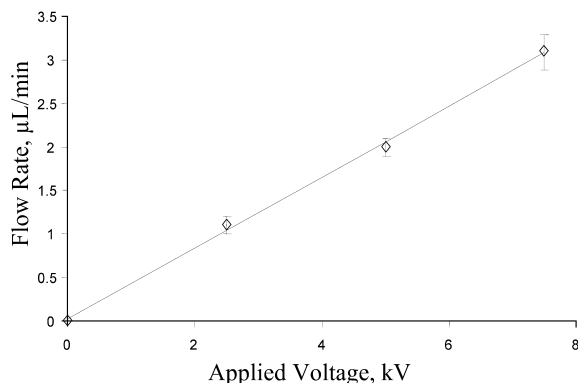

Fig. 5. Effect of applied voltage on pumping rate. A 20-cm-long backpressure capillary is attached to the pump used in Fig. 3 for this experiment. The diamond marks represent the measured pumping rates when the voltages applied across the pump channels are 2.5, 5 and 7.5 kV. The point at the origin is taken as granted (not measured). All other experimental conditions are the same as those in Fig. 3. The solid line is calculated using Eq. (7). See the text for details regarding the parameters used for the calculation.
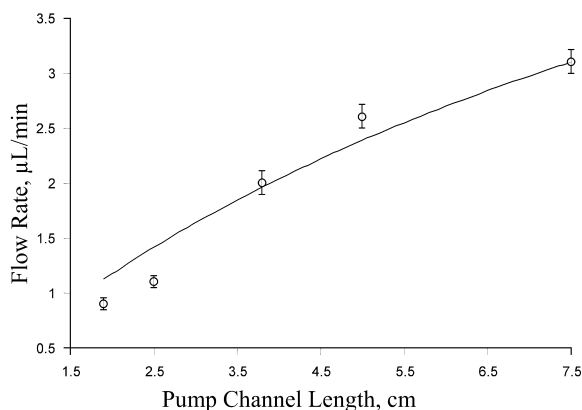
Fig. 6. Effect of pump channel length on pumping rate.. Five different pump devices are used in this experiment. All the devices contain 32 pump channels but their channel lengths are 18.75, 25, 37.5, 50 and 75 mm, respectively. See Fig. 1 for their photomask design. A 10-cm-long backpressure capillary is attached to each pump device for the experiment. All other experimental conditions are the same as those in Fig. 3. The circles indicate the pump rates obtained from different pump devices. The solid line is calculated based on Eq. (7).

to that of the pump solution (pH~9.2). A 2 cm×250 μm I.D. capillary was used to facilitate the flow-rate measurement without introducing significant back-pressure.
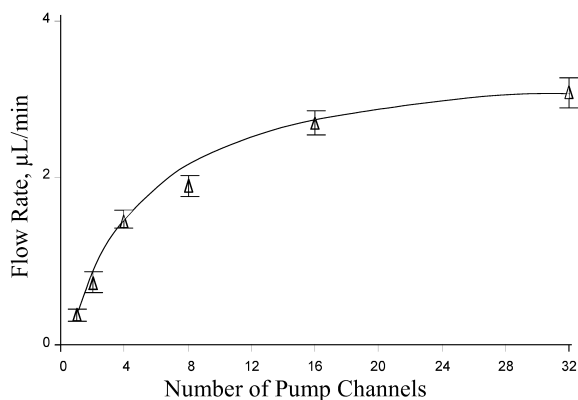

Fig. 7. Flow rate as a function of the number of pump channels. Six different pump devices are used in this experiment. All pump channels have the same length but each device contains a different number (1, 2, 4, 8, 16 or 32) of pump channels. See Fig. 1 for their photomask design. A 10-cm-long backpressure capillary is attached to each pump device for the experiment. All other experimental conditions are the same as those in Fig. 3. The triangle symbols represent the pump rates obtained from different pump devices. The solid line is calculated using Eq. (7).
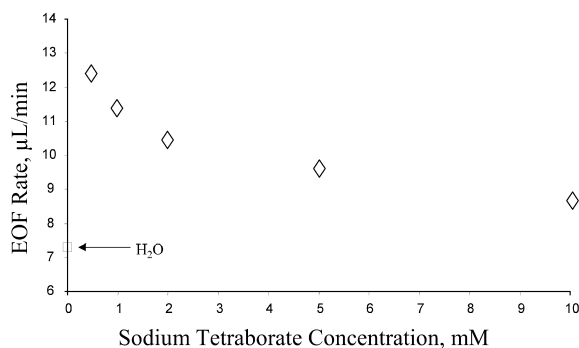

Fig. 8. Effect of borax concentration on EOF. The pump device used in this experiment is the same as that in Fig. 3. The backpressure capillary is a 2-cm-long and 250-μm-I.D. capillary to facilitate the pump solution collection. For the test, 0.5, 1-, 2-, 5- and 10-mM sodium tetraborate solutions are used. The measurement is carried out from low to high concentrations of the sodium tetraborate. All other experimental conditions are the same as those in Fig. 3. The square symbol represents the EOF rate at zero borax concentration (de-ionized water).

From Eqs. (2) and (7), the overall flow rate, Q_c, can be rewritten as,

$$Q_c = \frac{3\pi L'd^4}{1 + 32nLwd'^3} \cdot Q_{eo} \tag{11}$$

Q_c is directly proportional to the Q_{eo}. Therefore, any factor that affects EOF will influence the overall flow rate proportionally.

5. Conclusions

We have demonstrated the feasibility of an electric field-decoupled and stand-alone pump for microfluidic systems. A theoretical model has been developed to estimate the overall pump rate and its validity has been experimentally examined. The pump rates calculated based on the model have matched the measured flow rates very well. The theory has included many experimental parameters, such as the pump channel length and depth, the number of pump channels, the pump load or the backpressure, the field strength applied to the pump channel and the factors affecting EOF of the pump channels. Therefore, the theoretical model can pro-

vide some guidelines to design pumps for microfluidic systems.

The characteristics of an EOF-based pump are pulse-free flow, instant flow start and stop (the EOF starts or stops almost instantly as the HV power supply is turned on or off), and precise movement of fluid at sub-μl to pl volume levels. All these characteristics are excellent for pipetting, transfer and delivery of very small volumes of reagents and samples. The samples and reagents dealt with in microfluidic and nanofluidic devices are normally within these volume levels. Therefore, EOF-based pumps will be particularly useful to precisely move fluid in these devices. A sub-μl pipette can also be constructed using EOF pumping to pipet, transfer and deliver solutions of sub-μl to pl volume levels. However, the advantages of EOF-based pumps will be diminished if the desired flow rate is high (e.g. greater than 100 μl per min) because Joule heating increases with the EOF rate. The pumping rate tends to drift if it is operated continuously in one direction for a long period of time (e.g. longer than 1 day) because electrolysis changes the pH of the pump solution.

Acknowledgements

References

[1] S. Liu, P.K. Dasgupta, Anal. Chim. Acta 268 (1992) 1.

[2] P.K. Dasgupta, S. Liu, Anal. Chem. 66 (1994) 1792.

[3] S. Liu, P.K. Dasgupta, Anal. Chim. Acta 283 (1993) 739.

[4] S. Liu, P.K. Dasgupta, Talanta 41 (1994) 1903.

[5] S. Liu, P.K. Dasgupta, Anal. Chim. Acta. 308 (1995) 281.

[6] P.H. Paul, D.W. Arnold, D.J. Rakestraw, in: D.J. Harrison, A. van den Berg (Eds.), Micro Total Analysis Systems '98, Kluwer, Boston, MA, 1998, p. 49.

[7] P.H. Paul, D.W. Arnold, D.W. Neyer, K.B. Smith, in: A. van den Berg, W. Olthuis, P. Bergveld (Eds.), Micro Total Analysis Systems '2000, Kluwer, Boston, MA, 2000, p. 583.

[8] D.J. Harrison, K. Fluri, K. Seiler, Z.H. Fan, C.S. Effenhauser, A. Manz, Science 261 (1993) 895.

[9] S.C. Jacobson, R. Hergenroder, L.B. Koutny, J.M. Ramsey, Anal. Chem. 66 (1994) 1114.

[10] C.S. Effenhauser, G.J.M. Bruin, A. Paulus, Electrophoresis 18 (1997) 2203.

[11] H. Swerdlow, J.Z. Zhang, D.Y. Chen, H.R. Harke, R. Grey, S. Wu, N.J. Dovichi, C. Fuller, Anal. Chem. 63 (1991) 2835.

[12] Y. Takamura, H. Onoda, H. Inokuchi, S. Adachi, A. Oki, Y. Horiike, in: J.M. Ramsey, A. van den Berg (Eds.), Proceedings of the μTAS 2001 Symposium, 21–25 October, 2001, Kluwer, Dordrecht, The Netherlands, 2001, p. 230.

[13] I.M. Lazar, B.L. Karger, in: J.M. Ramsey, A. van den Berg (Eds.), Proceedings of the μTAS 2001 Symposium, 21–25 October, 2001, Kluwer, Dordrecht, The Netherlands, 2001, p. 219.

[14] I.M. Lazar, B.L. Karger, Anal. Chem. 74 (2002) 6259.

[15] S. Liu, H. Ren, Q. Gao, Q. Mao, D. Roach, R. Loder, T. Armstrong, I. Blaga, S. Jovanovich, D. Barker, Proc. Natl. Acad. Sci. USA 97 (2000) 5369.

[16] R.A. Wallingford, A.G. Ewing, Adv. Chromatogr. 29 (1989) 1.

[17] J.C. Giddings, in: Unified Separation Science, Wiley, New York, 1990, p. 60.

[18] R.B. Bird, W.E. Stewart, E.N. Lightfoot, Transport Phenomena, 2nd ed, Wiley–Interscience, New York, 2002.